
Real and Complex Models of Multi-phase Permanent Magnet Synchronous Motors

R. Zanasi, F. Grossi*, M. Fei

Department of Computer Science and Engineering,
Università di Modena e Reggio Emilia,
41125 Modena, Italy
E-mail: {roberto.zanasi, federica.grossi, marco.fei}@unimore.it,
*Corresponding author

Abstract: The paper deals with the modeling of multi-phase permanent magnet synchronous machines (PMSM) with an arbitrary number of phases and arbitrary shape of the rotor flux. The aim of the paper is to propose new dynamic models for the multi-phase electrical machines based on the use of real and complex state space transformations which are invariant with respect to power. The dynamic models of the motor are obtained using a Lagrangian approach in the frame of the Power-Oriented Graphs technique. The obtained dynamic models can directly be implemented in Simulink whatever the number of phase is. The state space transformations presented in the paper (both real and complex) are compared to the main other transformations known in the literature. Some simulation results are finally presented.

Keywords: Multi-phase synchronous motor, Modeling, Power-Oriented Graphs, State space transformation.

Reference to this paper should be made as follows: Zanasi, R., Grossi, F. and Fei, M. (2012) 'Real and Complex Models of Multi-phase Permanent Magnet Synchronous Motors', *Int. J. Power and Energy Conversion*, Vol., No., hpp..

Biographical notes: R. Zanasi graduated with honors in Electrical Engineering in 1986. Since 1998 he has been working as Associate Professor of Automatic Control at University of Modena and Reggio Emilia. In 2004 he became Professor in Automatic Control. He held the position of Visiting Scientist at the IRIMS of Moscow in 1991, at the MIT of Boston in 1992 and at the Université Catholique de Louvain in 1995. His research interests include: mathematical modeling, simulation, automotive, control of variable-structure systems, integral control, sliding mode control, robotics, etc.

Federica Grossi took her Master Degree cum laude in Electronic Engineering in 2006 and Ph.D. degree in 2010 in the domain of Dynamic Modeling and Control of Hybrid Automotive Systems at the University of Modena and Reggio Emilia. She has now a Post-Doc position with the Department of Information Engineering at the University of Modena. Her research interests include graphical modelling techniques applied to electro-mechanical systems and hybrid automotive systems.

Marco Fei received the Master Degree cum laude in Electronic Engineering from the University of Modena and Reggio Emilia in 2009. He is currently a Ph.D. student at the University of Modena and Reggio Emilia with the research topic “Dynamic Power Control of Hybrid Vehicles by using Multi-Phase Electric Motors”. His research interests include the modelling and the control of automotive and electro-mechanical systems.

1 Introduction

The dynamic model of three-phase synchronous machines is well known in the literature and usually some coordinate transformations White and Woodson (1959), named Park and Clarke, are exploited in order to write the equations of the system in a compact and suitable form. Some similar state space transformations can be exploited also in the case of multi-phase machines, where the number of phases is greater than three. Multi-phase machines offer some advantages compared to three-phase machines, see Levi (2008) and Parsa (2005). In the modeling of multi-phase machines a variety of transformations have been proposed, see Parsa and Toliyat (2005), Kestelyn et al. (2002), Semail et al. (2004), Paap (2000) and Toliyat et al. (1991). A first general formulation of the possible state space transformations has been given in Figueroa et al. (2006). In Parsa and Toliyat (2005) a pseudo orthogonal transformation is introduced to simplify the model of a five-phase machine and the original five-dimensional space is mapped into two two-dimensional orthogonal subspaces. In Kestelyn et al. (2002) the equivalence of a m -phase wye-connected machine to a set of $(m - 1)/2$ fictitious independent two-phase machines is shown. This concept is also used in Semail et al. (2004) in the case of five-phase machine.

In this paper three different “congruent” transformations (both real and complex) for modeling multi-phase PMSM are proposed. They are suitable for machines with an arbitrary odd number of stator phases and for arbitrary shape of the rotor flux. Such transformations are in bijective correspondence each other and therefore they are equivalent. The advantages of using these transformations will be discussed in the paper, together with a comparison with the main classical transformations, see White and Woodson (1959), Grandi et al. (2006), Fortescue (1918), Clarke (1950) and Park (1929).

The dynamic models of multi-phase PMSM known in the literature are usually obtained using classical mathematical methods Vas (1990), Leonhard (2001). In this paper the models are obtained using a Lagrangian approach in the frame of the Power-Oriented Graphs (POG) technique, see Zanasi and Grossi (2008). This graphical modeling technique shows the power flows within the system, allows to write the state space equations of the system in a very compact form and provides a power-invariant model which can be directly implemented in Simulink. With the proposed transformations the dynamics of the system can be written in a very compact and simple form.

The paper is organized as follows. Sec. 2 introduces the main features of POG technique, Sec. 3 shows the details of the POG dynamic model of the multi-phase

PMSM, Sec. 4 deals with the proposed coordinate transformations compared with classical transformations and Sec. 5 reports some simulation results. Finally some conclusion are drawn in Sec. 6.

2 Power-Oriented Graphs basic principles

The Power-Oriented Graphs technique, see Zanasi (1991) and Zanasi (2010), is an energy-based technique suitable for modeling physical systems. The POG are block diagrams combined with a particular modular structure essentially based on the use of the two blocks shown in Fig. 1.a and Fig. 1.b: the *elaboration block* (e.b.) stores and/or dissipates energy (i.e. springs, masses, dampers, capacities, inductances, resistances, etc.), the *connection block* (c.b.) redistributes the power within the system without storing nor dissipating energy (i.e. any type of gear reduction, transformers, etc.). The c.b. transforms the power variables with the constraint $\mathbf{x}_1^* \mathbf{y}_1 = \mathbf{x}_2^* \mathbf{y}_2$. The e.b. and the c.b. are suitable for representing both scalar and vectorial systems. In the vectorial case, $\mathbf{G}(s)$ and \mathbf{K} are matrices: $\mathbf{G}(s)$ is always square, \mathbf{K} can also be rectangular. The circle present in the e.b. is a summation element and the black spot represents a minus sign that multiplies the entering variable. The main feature of the Power-Oriented Graphs is to keep a direct correspondence between the dashed sections of the graphs and real power sections of the modeled system: the scalar product $\mathbf{x}^* \mathbf{y}$ of the two *power vectors* \mathbf{x} and \mathbf{y} involved in each dashed line of a Power-Oriented Graphs, see Fig. 1, has the physical meaning of the *power flowing through that particular section*.

Another important aspect of the POG technique is the direct correspondence between the POG representations and the corresponding state space descriptions. For example, the POG scheme shown in Fig. 1.c can be represented by the state space equations given in (1) where the *energy matrix* \mathbf{L} is symmetric and positive definite: $\mathbf{L} = \mathbf{L}^* > 0$. For such a system, the stored energy E_s and the dissipating power P_d can always be expressed as follows: $E_s = \frac{1}{2} \mathbf{x}^* \mathbf{L} \mathbf{x}$, $P_d = \mathbf{x}^* \mathbf{A} \mathbf{x}$.

The dynamic model (1) can be transformed and reduced into system (2) using a “congruent” transformation $\mathbf{x} = \mathbf{T} \mathbf{z}$ (matrix \mathbf{T} can be rectangular and time-varying) where $\bar{\mathbf{L}} = \mathbf{T}^* \mathbf{L} \mathbf{T}$, $\bar{\mathbf{A}} = \mathbf{T}^* \mathbf{A} \mathbf{T} + \mathbf{T}^* \mathbf{L} \dot{\mathbf{T}}$ and $\bar{\mathbf{B}} = \mathbf{T}^* \mathbf{B}$.

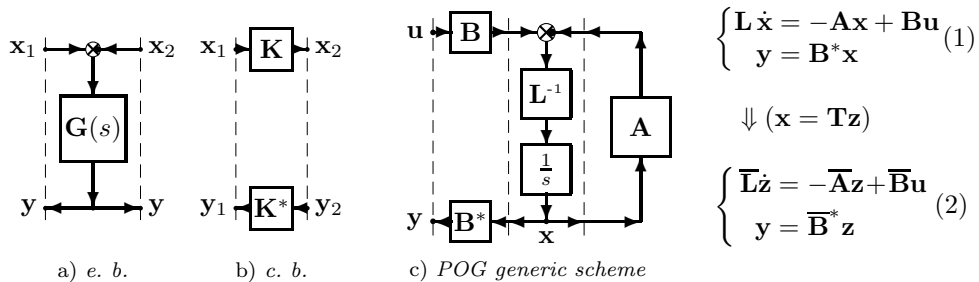


Figure 1 POG basic blocks: a) *elaboration block*; b) *connection block*. c) POG scheme of a generic dynamic system in the complex domain.

2.1 Notations

The full and diagonal matrices and the column and row vectors will be denoted as:

$$\begin{aligned} \begin{bmatrix} R_{11} & R_{12} & \cdots & R_{1m} \\ R_{21} & R_{22} & \cdots & R_{2m} \\ \vdots & \vdots & \ddots & \vdots \\ R_{n1} & R_{n2} & \cdots & R_{nm} \end{bmatrix}, \quad \begin{bmatrix} R_1 \\ R_2 \\ \vdots \\ R_n \end{bmatrix}, \quad \begin{bmatrix} R_1 \\ R_2 \\ \vdots \\ R_n \end{bmatrix}, \quad \begin{bmatrix} R_1 & R_2 & \cdots & R_n \end{bmatrix}. \end{aligned}$$

The symbol $\sum_{n=a:d}^b c_n = c_a + c_{a+d} + c_{a+2d} + \dots$ will be used to represent the sum of a succession of numbers c_n where the index n ranges from a to b with increment d , that is, using the Matlab symbology, $n = [a : d : b]$. Given a complex matrix \mathbf{A} , the conjugate matrix will be denoted by \mathbf{A}° , the transpose matrix by \mathbf{A}^\top and the conjugate transpose matrix by \mathbf{A}^* . The following relations hold: $\mathbf{A}^* = (\mathbf{A}^\circ)^\top = (\mathbf{A}^\top)^\circ$. The symbol $\mathbf{0}$ will be used to indicate a zero block matrix of proper dimensions.

3 Electrical motors modeling

The basic structure of a multi-phase PMSM is shown in Fig. 2. In this paper we refer to a PMSM with an *odd* number m_s of concentrated windings, see Zanasi and Grossi (2008), characterized by the parameters shown in Tab. 1. Saturation of iron will be neglected in this analysis. Let us introduce the following current and voltage stator vectors: ${}^t\mathbf{I}_s = [I_{s1} \ I_{s2} \ \cdots \ I_{sm_s}]^\top$, ${}^t\mathbf{V}_s = [V_{s1} \ V_{s2} \ \cdots \ V_{sm_s}]^\top$. Using a ‘‘Lagrangian’’ approach, see Zanasi and Grossi (2008), the dynamic model S_t of the considered electric motor with respect to the external fixed frame Σ_t is the following:

$$\begin{bmatrix} {}^t\mathbf{L}_s & \mathbf{0} \\ \mathbf{0} & J_m \end{bmatrix} \begin{bmatrix} \dot{{}^t\mathbf{I}}_s \\ \dot{\omega}_m \end{bmatrix} = - \begin{bmatrix} {}^t\mathbf{R}_s & {}^t\mathbf{K}_\tau(\theta) \\ -{}^t\mathbf{K}_\tau^\top(\theta) & b_m \end{bmatrix} \begin{bmatrix} {}^t\mathbf{I}_s \\ \omega_m \end{bmatrix} + \begin{bmatrix} {}^t\mathbf{V}_s \\ -\tau_e \end{bmatrix} \quad (3)$$

where the resistance matrix is ${}^t\mathbf{R}_s = R_s \mathbf{I}_{m_s}$ and the inductance matrix is defined

as: ${}^t\mathbf{L}_s = L_{s0} \mathbf{I}_{m_s} + M_{s0} \begin{bmatrix} \cos((i-h)\gamma_s) \\ \vdots \end{bmatrix}_{1:m_s}^i$, with $L_{s0} = L_s - M_{s0}$. According to the

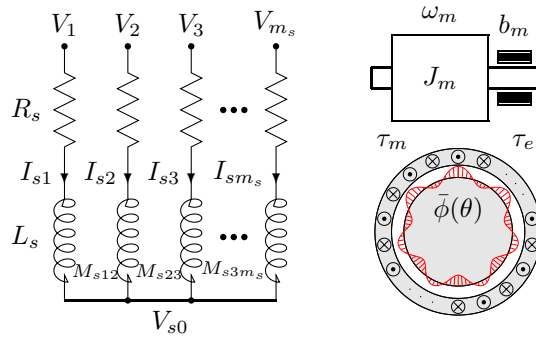


Figure 2 Basic structure of a multi-phase PMSM.

m_s	number of motor phases
p	number of polar expansions
θ, θ_m	electric and rotor angular positions: $\theta = p \theta_m$
ω, ω_m	electric and rotor angular velocities: $\omega = p \omega_m$
R_s	i -th stator phase resistance
L_s	i -th stator phase self induction coefficient
M_{s0}	maximum value of mutual inductance
$\phi_c(\theta)$	total rotor flux chained with stator phase 1
φ_c	maximum value of function $\phi_c(\theta)$
J_m	rotor moment of inertia
b_m	rotor linear friction coefficient
τ_m	electromotive torque acting on the rotor
τ_e	external load torque acting on the rotor
γ_s	basic angular displacement ($\gamma_s = 2\pi/m_s$)

Table 1 Main parameters of a multi-phase PMSM.

magnetic co-energy method the torque τ_m and the back-electromotive force ${}^t\mathbf{E}_s$ can be written as: $\tau_m = {}^t\mathbf{K}_\tau^T {}^t\mathbf{I}_s$ and ${}^t\mathbf{E}_s = {}^t\mathbf{K}_\tau \omega_m$ where the torque vector ${}^t\mathbf{K}_\tau(\theta)$ (also known as speed normalized back electromotive force vector) is:

$${}^t\mathbf{K}_\tau(\theta) = \frac{\partial {}^t\Phi_c(p\theta_m)}{\partial \theta_m} = p \varphi_c \left[\left[- \sum_{\substack{n=1:2 \\ 0:m_s-1}}^{\infty} n a_n \sin(n(\theta - h\gamma_s)) \right] \right]. \quad (4)$$

Note that the rotor flux linkage vector $\Phi_c(\theta)$ is expressed in Fourier expansion:

$$\Phi_c(\theta) = \varphi_c \left[\left[\bar{\phi}(\theta - h\gamma) \right] \right] = \varphi_c \left[\left[\sum_{\substack{n=1:2 \\ 0:m-1}}^{\infty} a_n \cos[n(\theta - h\gamma_s)] \right] \right]. \quad (5)$$

The POG block scheme of the PMSM in the fixed reference frame Σ_t , see eq. (3), is shown in Fig. 3. The POG scheme clearly puts in evidence four different power sections. The *elaboration blocks* between the power sections ① and ② represent the *Electrical part* of the system, while the blocks between sections ③ and ④ represent the *Mechanical part* of the system. The *connection block* between sections ② and ③ represents the energy and power conversion (without accumulation nor dissipation) between the electrical and mechanical parts of the motor.

4 State Space Transformations

In this section three different state space transformations will be presented and the corresponding three different and equivalent dynamic models of the motor will be obtained. A comparison with the main transformations typically used in the literature is also given.

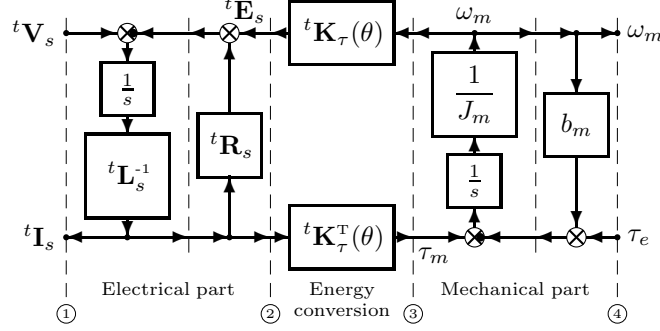


Figure 3 POG block scheme of the dynamic model of a multi-phase PMSM in the fixed reference frame Σ_t .

4.1 System S_ω in the rotating frame Σ_ω

The dynamic model (3) of the multi-phase PMSM can be expressed in a rotating frame Σ_ω using a state space transformation ${}^t\mathbf{I}_s = {}^t\mathbf{T}_\omega {}^\omega\mathbf{I}_s$ based on the orthonormal matrix: ${}^t\mathbf{T}_\omega = \begin{bmatrix} {}^t\mathbf{T}_\omega & \mathbf{z}_{m_s} \end{bmatrix} \in \mathbb{R}^{m_s \times m_s}$, where matrix ${}^t\mathbf{T}_\omega \in \mathbb{R}^{m_s \times (m_s-1)}$ and vector $\mathbf{z}_{m_s} \in \mathbb{R}^{m_s}$ have the form:

$${}^t\mathbf{T}_\omega = \sqrt{\frac{2}{m_s}} \begin{bmatrix} \cos(k(h\gamma_s - \theta)) & \sin(k(h\gamma_s - \theta)) \end{bmatrix}_{0:m_s-1}^h, \quad \mathbf{z}_{m_s} = \begin{bmatrix} \sqrt{\frac{1}{m_s}} \end{bmatrix}_{0:m_s-1}^h. \quad (6)$$

When the stator phases are star-connected, the last column of matrix ${}^t\mathbf{T}_\omega$ can be eliminated and matrix ${}^t\mathbf{T}_\omega$ reduces to the rectangular matrix ${}^t\mathbf{T}_\omega$. Matrix ${}^t\mathbf{T}_\omega(\theta)$ is a function of the electrical angle θ and transforms the system variables from the original reference frame Σ_t to a transformed rotating frame Σ_ω . For $m_s = 5$ the transformation matrix ${}^t\mathbf{T}_\omega$ is:

$${}^t\mathbf{T}_\omega = \sqrt{\frac{2}{5}} \begin{bmatrix} \cos(-\theta) & \sin(-\theta) & \cos(-3\theta) & \sin(-3\theta) & \frac{1}{\sqrt{2}} \\ \cos(\gamma_s - \theta) & \sin(\gamma_s - \theta) & \cos(3\gamma_s - 3\theta) & \sin(3\gamma_s - 3\theta) & \frac{1}{\sqrt{2}} \\ \cos(2\gamma_s - \theta) & \sin(2\gamma_s - \theta) & \cos(6\gamma_s - 3\theta) & \sin(6\gamma_s - 3\theta) & \frac{1}{\sqrt{2}} \\ \cos(3\gamma_s - \theta) & \sin(3\gamma_s - \theta) & \cos(9\gamma_s - 3\theta) & \sin(9\gamma_s - 3\theta) & \frac{1}{\sqrt{2}} \\ \cos(4\gamma_s - \theta) & \sin(4\gamma_s - \theta) & \cos(12\gamma_s - 3\theta) & \sin(12\gamma_s - 3\theta) & \frac{1}{\sqrt{2}} \end{bmatrix}_{m_s}^h.$$

Applying the congruent state space transformation ${}^t\mathbf{I}_s = {}^t\mathbf{T}_\omega {}^\omega\mathbf{I}_s$ to system (3), one obtains the following transformed system S_ω expressed in the rotating frame Σ_ω :

$$\begin{bmatrix} \frac{\omega}{J_m} \mathbf{L}_s & \mathbf{0} \\ \mathbf{0} & \frac{\omega}{J_m} \end{bmatrix} \begin{bmatrix} \frac{\omega}{J_m} \mathbf{I}_s \\ \dot{\omega}_m \end{bmatrix} = - \begin{bmatrix} \frac{\omega}{J_m} \mathbf{R}_s + \frac{\omega}{J_m} \mathbf{L}_s \frac{\omega}{J_m} \mathbf{J}_s & \frac{\omega}{J_m} \mathbf{K}_\tau(\theta) \\ -\frac{\omega}{J_m} \mathbf{K}_\tau^T(\theta) & b_m \end{bmatrix} \begin{bmatrix} \frac{\omega}{J_m} \mathbf{I}_s \\ \omega_m \end{bmatrix} + \begin{bmatrix} \frac{\omega}{J_m} \mathbf{V}_s \\ -\tau_e \end{bmatrix}. \quad (7)$$

The POG scheme of the multi-phase PMSM in rotating frame Σ_ω , see (7), is shown in Fig. 4. The *connection block* between sections ① and ① represents the state space transformation ${}^t\mathbf{T}_\omega$ between the fixed reference frame Σ_t and the rotating

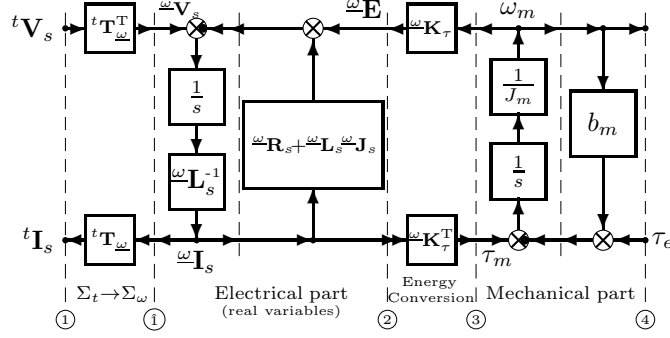


Figure 4 POG scheme of a PMSM in rotating frame Σ_ω .

reference frame Σ_ω . The transformed diagonal resistance matrix is not modified $\underline{\omega}\mathbf{R}_s = {}^t\mathbf{T}_\omega^T {}^t\mathbf{R}_s {}^t\mathbf{T}_\omega = {}^t\mathbf{R}_s$, while the inductance and coupling square matrices $\underline{\omega}\mathbf{L}_s$ and $\underline{\omega}\mathbf{J}_s$ have the following simplified structure:

$$\underline{\omega}\mathbf{L}_s = {}^t\mathbf{T}_\omega^T {}^t\mathbf{L}_s {}^t\mathbf{T}_\omega = \begin{bmatrix} \begin{bmatrix} L_{sk} & 0 \\ 0 & L_{sk} \end{bmatrix} & \mathbf{0} \\ \mathbf{0} & L_{s0} \end{bmatrix}, \quad \underline{\omega}\mathbf{J}_s = {}^t\mathbf{T}_\omega^T {}^t\mathbf{J}_s {}^t\mathbf{T}_\omega = \begin{bmatrix} \begin{bmatrix} 0 & -k\omega \\ k\omega & 0 \end{bmatrix} & \mathbf{0} \\ \mathbf{0} & 0 \end{bmatrix},$$

where L_{sk} is:

$$L_{sk} = \begin{cases} L_{s0} + \frac{m_s}{2} M_{s0} & \text{for } k = 1 \\ L_{s0} & \text{for } k \in \{3, 5, \dots, m_s - 2\} \end{cases} \quad (8)$$

The transformed current and voltage vectors $\underline{\omega}\mathbf{I}_s = {}^t\mathbf{T}_\omega^T {}^t\mathbf{I}_s$ and $\underline{\omega}\mathbf{V}_s = {}^t\mathbf{T}_\omega^T {}^t\mathbf{V}_s$ in (7) are defined as:

$$\underline{\omega}\mathbf{I}_s = \begin{bmatrix} \begin{bmatrix} \omega I_{dk} & \omega I_{qk} \end{bmatrix}^k \\ \omega I_{sm_s} \end{bmatrix}^T, \quad \underline{\omega}\mathbf{V}_s = \begin{bmatrix} \begin{bmatrix} \omega V_{dk} & \omega V_{qk} \end{bmatrix}^k \\ \omega V_{sm_s} \end{bmatrix}^T \quad (9)$$

where ωI_{dk} , ωI_{qk} , ωV_{dk} and ωV_{qk} are, respectively, the *direct* and *quadrature* components of the current and voltage vectors $\underline{\omega}\mathbf{I}_s$ and $\underline{\omega}\mathbf{V}_s$ in the rotating reference frame Σ_ω . The last components ωI_{sm_s} and ωV_{sm_s} are proportional to the sum of the m_s stator currents I_{sh} and the m_s stator voltages V_{sh} , respectively:

$$\omega I_{sm_s} = \mathbf{z}_{m_s}^T {}^t\mathbf{I}_s = \sqrt{\frac{1}{m_s}} \sum_{h=1}^{m_s} I_{sh}, \quad \omega V_{sm_s} = \mathbf{z}_{m_s}^T {}^t\mathbf{V}_s = \sqrt{\frac{1}{m_s}} \sum_{h=1}^{m_s} V_{sh}. \quad (10)$$

Note that it is ${}^\omega I_{sm_s} = 0$ when the stator phases are star-connected and ${}^\omega V_{sm_s} = 0$ when the input stator voltages are balanced. The transformed torque vector ${}^\omega \mathbf{K}_\tau(\theta) = {}^t \mathbf{T}_\omega^T {}^t \mathbf{K}_\tau(\theta)$ in the rotating frame Σ_ω is (see Zanasi and Grossi (2008)):

$${}^\omega \mathbf{K}_\tau(\theta) = \begin{bmatrix} k \\ \left[\begin{array}{c} \omega K_{dk} \\ \omega K_{qk} \end{array} \right]_{1:2:m_s-2} \\ \omega K_{\tau m_s} \end{bmatrix} = p \varphi_c \sqrt{\frac{m_s}{2}} \begin{bmatrix} \left[\begin{array}{c} \sum_{n=0:2m_s}^{\infty} -[(n+k)a_{n+k} + (n-k)a_{n-k}] \sin(n\theta) \\ \sum_{n=0:2m_s}^{\infty} [(n+k)a_{n+k} - (n-k)a_{n-k}] \cos(n\theta) \end{array} \right]_{1:2:m_s-2} \\ -\sqrt{2} \sum_{n=m_s:2m_s}^{\infty} n a_n \sin(n\theta) \end{bmatrix} \quad (11)$$

This expression of the torque vector ${}^\omega \mathbf{K}_\tau$ can be used for any shape of the normalized rotor flux $\bar{\phi}(\theta)$, it can be easily computed knowing the coefficients a_n of the flux Fourier expansion (5) and it is constant (not function of the electric angle θ) only for the following normalized flux functions $\bar{\phi}(\theta)$:

$$\bar{\phi}(\theta) = \sum_{i=1:2}^{m_s-2} a_i \cos(i\theta). \quad (12)$$

When the rotor flux has the shape given in (12) the constant torque vector ${}^\omega \mathbf{K}_\tau$ has the following form:

$${}^\omega \mathbf{K}_\tau(\theta) = {}^\omega \mathbf{K}_\tau = p \varphi_c \sqrt{\frac{m_s}{2}} \begin{bmatrix} k \\ \left[\begin{array}{c} 0 \\ k a_k \end{array} \right]_{1:2:m_s-2} \\ 0 \end{bmatrix}. \quad (13)$$

This expression shows that the motor torque $\tau_m = {}^\omega \mathbf{K}_\tau^T {}^\omega \mathbf{I}_s$ depends only on the *quadrature* components ${}^\omega I_{qk}$ of the current vector ${}^\omega \mathbf{I}_s$. Note that (13) holds for a generic number of phases m_s , while usually in the literature only some particular cases for the torque vector ${}^\omega \mathbf{K}_\tau$ can be found, see for example Parsa and Toliyat (2005) and Shan et al. (2006).

The presented congruent state space transformation ${}^t \mathbf{I}_s = {}^t \mathbf{T}_\omega {}^\omega \mathbf{I}_s$ splits the original system S_t into $(m_s-1)/2$ two-dimensional orthogonal and decoupled subspaces, then the m_s -phase motor can be seen as a set of $(m_s-1)/2$ independent electrical machines rotating at different velocity $k p \omega_m$, each one working within a complex subspace $\bar{\Sigma}_{\omega k}$ with $k \in \{1:2:m_s-2\}$ and characterized by the k -th coefficient a_k of the rotor flux. The transformed system S_ω is described by means of real variables. Let $p(t) = {}^t \mathbf{V}_s^T {}^t \mathbf{I}_s$ and $s(t) = {}^\omega \mathbf{V}_s^T {}^\omega \mathbf{I}_s$ denote the instantaneous powers in sections ① and ① of the POG scheme in Fig. 4. It can be easily proved that the congruent transformation ${}^t \mathbf{T}_\omega$ is *power-invariant*, indeed the power $p(t)$ in section ① is equal to the power $s(t)$ in section ①:

$$p(t) = {}^t \mathbf{V}_s^T {}^t \mathbf{I}_s = {}^\omega \mathbf{V}_s^T {}^t \mathbf{T}_\omega^T {}^t \mathbf{T}_\omega {}^\omega \mathbf{I}_s = {}^\omega \mathbf{V}_s^T {}^\omega \mathbf{I}_s = s(t)$$

Comparison with Park and Clarke transformations. The transformation ${}^t\mathbf{T}_\omega$ is similar to the *Park transformation* typically used in the literature and also known as *dq0* transformation, see White and Woodson (1959). The generalized Park transformation is based on the following matrix $\underline{\omega}\mathbf{P}_t = {}^t\mathbf{P}_\omega^{-1} =$

$$\frac{2}{m_s} \begin{bmatrix} k \\ \left[\begin{array}{c} \cos(k(h\gamma_s - \theta)) \\ \sin(k(h\gamma_s - \theta)) \end{array} \right]_{1:2:m_s-2} \\ h \\ \left[\begin{array}{c} c \\ c \end{array} \right]_{0:m_s-1} \end{bmatrix} = \frac{2}{5} \begin{bmatrix} \cos(-\theta) & \cos(\gamma_s - \theta) & \cos(2\gamma_s - \theta) & \cos(3\gamma_s - \theta) & \cos(4\gamma_s - \theta) \\ \sin(-\theta) & \sin(\gamma_s - \theta) & \sin(2\gamma_s - \theta) & \sin(3\gamma_s - \theta) & \sin(4\gamma_s - \theta) \\ \cos(-3\theta) & \cos(3\gamma_s - 3\theta) & \cos(6\gamma_s - 3\theta) & \cos(9\gamma_s - 3\theta) & \cos(12\gamma_s - 3\theta) \\ \sin(-3\theta) & \sin(3\gamma_s - 3\theta) & \sin(6\gamma_s - 3\theta) & \sin(9\gamma_s - 3\theta) & \sin(12\gamma_s - 3\theta) \\ c & c & c & c & c \end{bmatrix}_{m_s}$$

where c is a constant: $c = \frac{1}{\sqrt{2}}$ in Parsa and Toliyat (2005) and $c = \frac{1}{2}$ in Shan et al. (2006). The Clarke transformation $\underline{\omega}\mathbf{C}_t$ (see White and Woodson (1959) and Clarke (1950)) can be obtained as a particular case from the Park transformation putting $\theta = 0$. Applying the Park similarity transformation ${}^P\mathbf{I}_s = {}^t\mathbf{P}_\omega^{-1} {}^t\mathbf{I}_s$ to system (3), one obtains an equivalent transformed system expressed in a rotating frame. Matrices ${}^t\mathbf{P}_\omega$ and ${}^t\mathbf{T}_\omega$ are related by the following relations:

$${}^t\mathbf{P}_\omega^{-1} = \mathbf{A} {}^t\mathbf{T}_\omega^T, \quad {}^t\mathbf{P}_\omega = \mathbf{A}^{-1} {}^t\mathbf{T}_\omega, \quad \text{with } \mathbf{A} = \sqrt{\frac{2}{m_s}} \begin{bmatrix} \mathbf{I}_{m_s-1} & \mathbf{0} \\ \mathbf{0} & \frac{1}{\sqrt{2}c} \end{bmatrix} \quad (14)$$

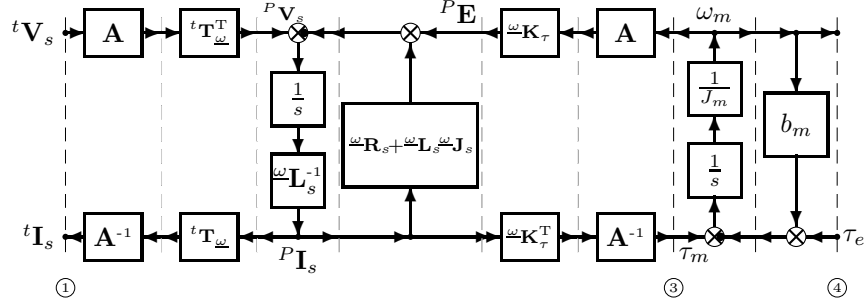
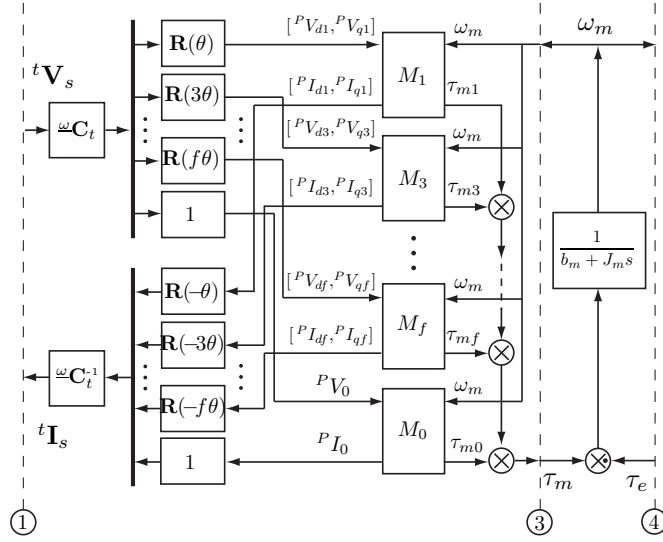
where the conversion matrix \mathbf{A} is needed to adjust the power. Indeed one can verify that the Park similarity transformation *is not power-invariant* because the instantaneous powers $p(t) = {}^t\mathbf{V}_s^T {}^t\mathbf{I}_s$ and $s(t) = {}^P\mathbf{V}_s^T {}^P\mathbf{I}_s$ are related as follows:

$$p(t) = (\mathbf{A}^{-1})^2 s(t) = \frac{m_s}{2} {}^P\mathbf{V}_s^T {}^P\mathbf{I}_s - \left(\frac{m_s}{2} - \frac{m_s}{4c^2} \right) {}^PV_0 {}^PI_0$$

where PV_0 and PI_0 are the last components of the voltage and current vectors ${}^P\mathbf{V}_s$ and ${}^P\mathbf{I}_s$, respectively. In case of star-connected phases the last column of matrix ${}^t\mathbf{P}_\omega^{-1}$ can be eliminated, so the relation between the matrices ${}^t\mathbf{P}_\omega$, ${}^t\mathbf{T}_\omega$ and the instantaneous powers $p(t)$ and $s(t)$ can be rewritten as:

$${}^t\mathbf{P}_\omega^{-1} = \sqrt{\frac{2}{m_s}} {}^t\mathbf{T}_\omega^T, \quad {}^t\mathbf{P}_\omega = \sqrt{\frac{m_s}{2}} {}^t\mathbf{T}_\omega, \quad p(t) = \frac{m_s}{2} s(t). \quad (15)$$

Fig. 5 shows a “POG-like” scheme of the electrical motor obtained with the Park transformation. Note that this scheme is similar to the POG scheme of Fig. 4 but the part between power sections ① and ③ does not keep the meaning of power because the Park similarity transformation *is not power-invariant*. The main disadvantage of using this transformation is that a particular conversion matrix \mathbf{A} and its inverse \mathbf{A}^{-1} are needed. On the contrary considering a power invariant transformation the meaning of power is kept even in the transformed system. The block scheme of Fig. 5 is equivalent to the block scheme of Fig. 6 typically used in the literature (see Semail et al. (2004)) where the $(m_s+1)/2$ fictitious machines are kept separated and the rotation matrix $\mathbf{R}(\theta)$ is defined as $\mathbf{R}(\theta) = \begin{bmatrix} \cos \theta & -\sin \theta \\ \sin \theta & \cos \theta \end{bmatrix}$. The scheme

**Figure 5** POG-like scheme of a m_s -phase motor in Park rotating frame.**Figure 6** Block scheme of a m_s -phase motor in Park rotating frame where $f = m_s - 2$ and block scheme of the k -th machine M_k for $k \in \{1 : 2 : f\}$.

given in Fig. 6 needs to be rearranged when the number of phases m_s changes while with the POG vectorial approach a unique general model is used whatever the number of phases m_s is. Moreover the system S_ω in Fig. 4 is obtained using a congruent transformation which uses the transpose of the transformation matrix (${}^t\mathbf{T}_\omega^T$) while the system in Fig. 6 is obtained using a similarity transformation which

uses the inverse of the transformation matrix (${}^t\mathbf{C}_\omega^{-1}$). The main features of the two transformations are summarized in the following Table:

Transf.	Power invariant	Dynamic equations	Fictitious machines	Variables	Vectorial notation
${}^t\mathbf{T}_\omega$	Yes	general m_s	$\frac{m_s+1}{2}$	real	Yes
${}^t\mathbf{P}_\omega$	No	fixed m_s	$\frac{m_s+1}{2}$	real	No

A very important advantage of exploiting the POG technique with vectorial notation is that the POG scheme of Fig. 4 can be directly implemented in Simulink without the need to consider separate fictitious machines. Moreover from the vectorial notation a better control can be implemented, as it will be shown in Section 5.

4.2 System \hat{S}_ω in the complex rotating frame $\hat{\Sigma}_\omega$

A complex dynamic model of the multi-phase PMSM expressed in a complex rotating frame $\hat{\Sigma}_\omega$ is obtained considering a state space transformation ${}^t\hat{\mathbf{I}}_s = {}^t\hat{\mathbf{T}}_\omega {}^\omega\mathbf{I}_s$ based on the complex orthonormal matrix ${}^t\hat{\mathbf{T}}_\omega = [{}^t\bar{\mathbf{T}}_\omega \ {}^t\bar{\mathbf{T}}_\omega^\circ \ \mathbf{z}_{m_s}] \in \mathbb{C}^{m_s \times m_s}$, where matrix ${}^t\bar{\mathbf{T}}_\omega \in \mathbb{C}^{m_s \times \frac{m_s-1}{2}}$ is:

$${}^t\bar{\mathbf{T}}_\omega = \sqrt{\frac{1}{m_s}} \begin{bmatrix} e^{jk(\theta - h\gamma_s)} \\ \vdots \\ e^{jk(\theta - (h-1)\gamma_s)} \end{bmatrix} \quad (16)$$

Matrix ${}^t\bar{\mathbf{T}}_\omega^\circ$ is the conjugate of matrix ${}^t\bar{\mathbf{T}}_\omega$ and vector \mathbf{z}_{m_s} is defined in (6). For $m_s = 5$ the transformation matrix ${}^t\hat{\mathbf{T}}_\omega$ has the following form:

$${}^t\hat{\mathbf{T}}_\omega = \frac{1}{\sqrt{5}} \begin{bmatrix} e^{j\theta} & e^{j3\theta} & e^{-j\theta} & e^{-j3\theta} & 1 \\ e^{j(\theta-\gamma_s)} & e^{j3(\theta-\gamma_s)} & e^{-j(\theta-\gamma_s)} & e^{-j3(\theta-\gamma_s)} & 1 \\ e^{j(\theta-2\gamma_s)} & e^{j3(\theta-2\gamma_s)} & e^{-j(\theta-2\gamma_s)} & e^{-j3(\theta-2\gamma_s)} & 1 \\ e^{j(\theta-3\gamma_s)} & e^{j3(\theta-3\gamma_s)} & e^{-j(\theta-3\gamma_s)} & e^{-j3(\theta-3\gamma_s)} & 1 \\ e^{j(\theta-4\gamma_s)} & e^{j3(\theta-4\gamma_s)} & e^{-j(\theta-4\gamma_s)} & e^{-j3(\theta-4\gamma_s)} & 1 \end{bmatrix}.$$

Applying the state space transformation ${}^t\hat{\mathbf{I}}_s = {}^t\hat{\mathbf{T}}_\omega {}^\omega\mathbf{I}_s$ to system (3), one obtains the following transformed system \hat{S}_ω in the complex rotating frame $\hat{\Sigma}_\omega$:

$$\begin{bmatrix} \frac{\omega\hat{\mathbf{L}}_s}{\mathbf{0}} \mid \mathbf{0} \\ \mathbf{0} \mid J_m \end{bmatrix} \begin{bmatrix} \frac{\omega\hat{\mathbf{I}}_s}{\dot{\omega}_m} \end{bmatrix} = - \begin{bmatrix} \frac{\omega\hat{\mathbf{R}}_s + \omega\hat{\mathbf{L}}_s \omega\hat{\mathbf{J}}_s}{-\omega\hat{\mathbf{K}}_\tau^*(\theta)} \mid \frac{\omega\hat{\mathbf{K}}_\tau(\theta)}{b_m} \end{bmatrix} \begin{bmatrix} \frac{\omega\hat{\mathbf{I}}_s}{\omega_m} \end{bmatrix} + \begin{bmatrix} \frac{\omega\hat{\mathbf{V}}_s}{-\tau_e} \end{bmatrix} \quad (17)$$

The POG scheme corresponding to the complex state space system (17) is shown in Fig. 7. The part of the block scheme between power sections ① and ③ is characterized by complex vectorial variables. Nevertheless, the scalar product of the complex variables involved in each dashed line of this part still has the physical meaning of

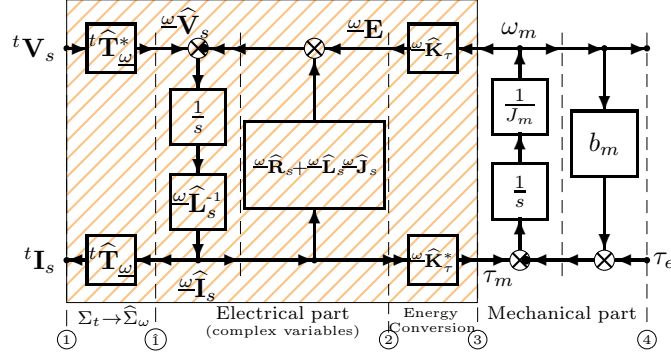


Figure 7 POG scheme of a PMSM in complex rotating frame $\hat{\Sigma}_\omega$.

instantaneous power flowing through that power section. The diagonal resistance matrix is not modified $\omega\hat{\mathbf{R}}_s = {}^t\hat{\mathbf{T}}_\omega^* {}^t\mathbf{R}_s {}^t\hat{\mathbf{T}}_\omega = {}^t\mathbf{R}_s$, while the complex inductance and coupling square matrices $\omega\hat{\mathbf{L}}_s$ and $\omega\hat{\mathbf{J}}_s$ have the following simplified structure:

$$\omega\hat{\mathbf{L}}_s = {}^t\hat{\mathbf{T}}_\omega^* {}^t\mathbf{L}_s {}^t\hat{\mathbf{T}}_\omega = \begin{bmatrix} \omega\bar{\mathbf{L}}_s & \mathbf{0} & \mathbf{0} \\ \mathbf{0} & \omega\bar{\mathbf{L}}_s^\circ & \mathbf{0} \\ \mathbf{0} & \mathbf{0} & L_{s0} \end{bmatrix}, \quad \omega\hat{\mathbf{J}}_s = {}^t\hat{\mathbf{T}}_\omega^* {}^t\hat{\mathbf{T}}_\omega = \begin{bmatrix} \omega\bar{\mathbf{J}}_s & \mathbf{0} & \mathbf{0} \\ \mathbf{0} & \omega\bar{\mathbf{J}}_s^\circ & \mathbf{0} \\ \mathbf{0} & \mathbf{0} & 0 \end{bmatrix} \quad (18)$$

where: $\omega\bar{\mathbf{L}}_s = \left[\begin{matrix} L_{sk} \\ 1:2:m_s-2 \end{matrix} \right]_k$, $\omega\bar{\mathbf{J}}_s = \left[\begin{matrix} jkp\omega_m \\ 1:2:m_s-2 \end{matrix} \right]_k$. The transformed complex

current and voltage vectors $\omega\hat{\mathbf{I}}_s$ and $\omega\hat{\mathbf{V}}_s$ have the following structure:

$$\omega\hat{\mathbf{I}}_s = {}^t\hat{\mathbf{T}}_\omega^* {}^t\mathbf{I}_s = \frac{1}{\sqrt{2}} \begin{bmatrix} \omega\bar{\mathbf{I}}_s \\ \omega\bar{\mathbf{I}}_s^\circ \\ \sqrt{2}\omega I_{sm_s} \end{bmatrix}, \quad \omega\hat{\mathbf{V}}_s = {}^t\hat{\mathbf{T}}_\omega^* {}^t\mathbf{V}_s = \frac{1}{\sqrt{2}} \begin{bmatrix} \omega\bar{\mathbf{V}}_s \\ \omega\bar{\mathbf{V}}_s^\circ \\ \sqrt{2}\omega V_{sm_s} \end{bmatrix} \quad (19)$$

where: $\omega\bar{\mathbf{I}}_s = \left[\begin{matrix} \omega\bar{I}_{sk} \\ 1:2:m_s-2 \end{matrix} \right]_k = \left[\begin{matrix} \omega I_{dk} + j\omega I_{qk} \\ 1:2:m_s-2 \end{matrix} \right]_k$, $\omega\bar{\mathbf{V}}_s = \left[\begin{matrix} \omega\bar{V}_{sk} \\ 1:2:m_s-2 \end{matrix} \right]_k = \left[\begin{matrix} \omega V_{dk} + j\omega V_{qk} \\ 1:2:m_s-2 \end{matrix} \right]_k$.

The components $\omega\bar{I}_{sk}$ and $\omega\bar{V}_{sk}$ of the vectors $\omega\bar{\mathbf{I}}_s$ and $\omega\bar{\mathbf{V}}_s$ are complex numbers where ωI_{dk} , ωI_{qk} , ωV_{dk} and ωV_{qk} are the *direct* and *quadrature* components of the current and voltage vectors defined in (9). The last components ωI_{sm_s} and ωV_{sm_s} of vectors $\omega\hat{\mathbf{I}}_s$ and $\omega\hat{\mathbf{V}}_s$ are defined in (10). The transformed torque vector $\omega\hat{\mathbf{K}}_\tau$ has the following structure:

$$\omega\hat{\mathbf{K}}_\tau(\theta) = {}^t\hat{\mathbf{T}}_\omega^* {}^t\mathbf{K}_\tau = \frac{1}{\sqrt{2}} \begin{bmatrix} \omega\bar{\mathbf{K}}_\tau \\ \omega\bar{\mathbf{K}}_\tau^\circ \\ \sqrt{2}\omega\bar{K}_{\tau m_s} \end{bmatrix} = \frac{1}{\sqrt{2}} \begin{bmatrix} \left[\begin{matrix} K_{dk} + jK_{qk} \\ 1:2:m_s-2 \end{matrix} \right]_k \\ \left[\begin{matrix} K_{dk} - jK_{qk} \\ 1:2:m_s-2 \end{matrix} \right]_k \\ \sqrt{2}\omega K_{\tau m_s} \end{bmatrix} \quad (20)$$

When the rotor flux function $\bar{\phi}(\theta)$ has the structure defined in (12) the complex torque vector $\underline{\omega}\hat{\mathbf{K}}_\tau$ is constant:

$$\underline{\omega}\hat{\mathbf{K}}_\tau^T(\theta) = \underline{\omega}\hat{\mathbf{K}}_\tau^T = p\varphi_c \sqrt{\frac{m_s}{4}} \begin{bmatrix} \left[\begin{smallmatrix} jka_k \\ 1:2:m_s-2 \end{smallmatrix} \right]^k \left[\begin{smallmatrix} -jka_k \\ 1:2:m_s-2 \end{smallmatrix} \right]^k 0 \end{bmatrix}.$$

Note that all the matrices $\underline{\omega}\hat{\mathbf{L}}_s$, $\underline{\omega}\hat{\mathbf{J}}_s$, $\underline{\omega}\hat{\mathbf{R}}_s$ and all the vectors $\underline{\omega}\hat{\mathbf{I}}_s$, $\underline{\omega}\hat{\mathbf{V}}_s$, $\underline{\omega}\hat{\mathbf{K}}_\tau$ of system (17) are block matrices and block vectors essentially composed by three blocks: the first two blocks have the same dimension $(m_s-1)/2$; the second block is the complex conjugate of the first one; the third block is a scalar real number.

The transformation ${}^t\hat{\mathbf{T}}_\omega$ is similar to the Fortescue transformation, also known as symmetrical transformation, see White and Woodson (1959) and Grandi et al. (2006), which is based on the following matrix:

$${}^t\mathbf{F}_\omega^* = \frac{1}{m_s} \begin{bmatrix} e^{j h k \gamma_s} \\ 0:m_s-1 \end{bmatrix}^k = \frac{1}{5} \begin{bmatrix} 1 & 1 & 1 & 1 & 1 \\ 1 & e^{j\gamma_s} & e^{j2\gamma_s} & e^{j3\gamma_s} & e^{j4\gamma_s} \\ 1 & e^{j2\gamma_s} & e^{j4\gamma_s} & e^{j6\gamma_s} & e^{j8\gamma_s} \\ 1 & e^{j3\gamma_s} & e^{j6\gamma_s} & e^{j9\gamma_s} & e^{j12\gamma_s} \\ 1 & e^{j4\gamma_s} & e^{j8\gamma_s} & e^{j12\gamma_s} & e^{j16\gamma_s} \end{bmatrix}_{\frac{m_s}{5}}$$

The system \hat{S}_ω is described by complex variables and it is obtained using an orthonormal congruent transformation. The transformed system \hat{S}_ω is decoupled in a set of $(m_s-1)/2$ electrical machines. Each electrical machine is described using vectors which are always composed by three elements, see (19), where the first two are conjugate to each other. The real and complex part of these transformed vectors are equal to the *direct* and *quadrature* components of the same vectors in the rotating frame Σ_ω . The transformation matrix ${}^t\hat{\mathbf{T}}_\omega$ is *power-invariant*. Indeed it can be easily proved that the instantaneous power $p(t) = {}^t\mathbf{V}_s^T {}^t\mathbf{I}_s$ in section ① of Fig. 7 is equal to the instantaneous power $s(t) = \underline{\omega}\hat{\mathbf{V}}_s^* \underline{\omega}\hat{\mathbf{I}}_s$ in section ②:

$$p(t) = {}^t\mathbf{V}_s^T {}^t\mathbf{I}_s = {}^t\mathbf{V}_s^* {}^t\mathbf{I}_s = \underline{\omega}\hat{\mathbf{V}}_s^* {}^t\hat{\mathbf{T}}_\omega^* {}^t\hat{\mathbf{T}}_\omega {}^t\omega\hat{\mathbf{I}}_s = \underline{\omega}\hat{\mathbf{V}}_s^* \underline{\omega}\hat{\mathbf{I}}_s = s(t).$$

The Fortescue transformation is *not power-invariant*, indeed the instantaneous powers $p(t) = {}^t\mathbf{V}_s^T {}^t\mathbf{I}_s$ and $s(t) = {}^F\mathbf{V}_s^T {}^F\mathbf{I}_s$ are not equal, but only proportional: $p(t) = m_s s(t)$.

4.3 System \bar{S}_ω in the reduced complex rotating frame $\bar{\Sigma}_\omega$

From (19) it follows that the real current vector ${}^t\mathbf{I}_s$ can be expressed as:

$$\begin{aligned} {}^t\mathbf{I}_s &= {}^t\hat{\mathbf{T}}_\omega \underline{\omega}\hat{\mathbf{I}}_s = \frac{1}{\sqrt{2}} \left({}^t\bar{\mathbf{T}}_\omega {}^\omega\bar{\mathbf{I}}_s + {}^t\bar{\mathbf{T}}_\omega {}^\omega\bar{\mathbf{I}}_s^* \right) + \mathbf{z}_{m_s} {}^\omega I_{sm_s} = \\ &= 2 \Re \left(\frac{1}{\sqrt{2}} {}^t\bar{\mathbf{T}}_\omega {}^\omega\bar{\mathbf{I}}_s \right) + \mathbf{z}_{m_s} {}^\omega I_{sm_s} = \Re \left(\sqrt{2} {}^t\bar{\mathbf{T}}_\omega {}^\omega\bar{\mathbf{I}}_s + \mathbf{z}_{m_s} {}^\omega I_{sm_s} \right) \quad (21) \\ &= \Re \left({}^t\bar{\mathbf{T}}_\omega \mathbf{N} \begin{bmatrix} {}^\omega\bar{\mathbf{I}}_s \\ {}^\omega I_{sm_s} \end{bmatrix} \right) \end{aligned}$$

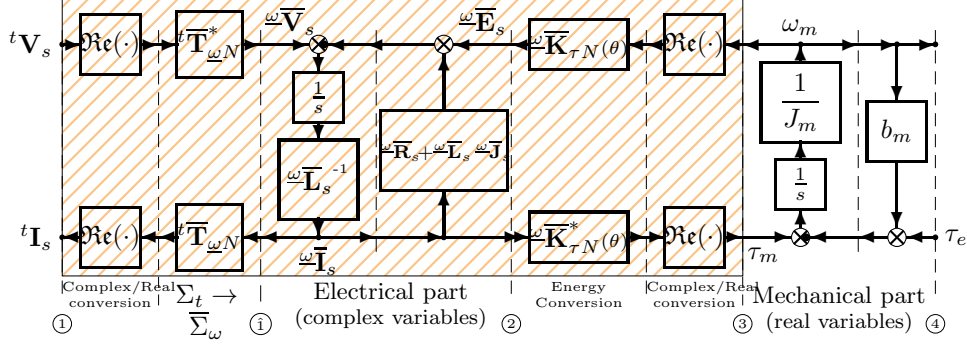


Figure 8 POG scheme of multi-phase PMSM in reduced complex rotating frame $\bar{\Sigma}_\omega$.

where: ${}^t\bar{\mathbf{T}}_\omega = [{}^t\bar{\mathbf{T}}_\omega \mathbf{z}_{m_s}]$, $\mathbf{N} = \begin{bmatrix} \sqrt{2}\mathbf{I}_{\frac{m_s-1}{2}} & \mathbf{0} \\ \mathbf{0} & 1 \end{bmatrix}$.

This relation shows that vector ${}^t\mathbf{I}_s$ can also be obtained without using the complex conjugate term ${}^t\bar{\mathbf{T}}_\omega \omega \bar{\mathbf{I}}_s$. Similarly it can be shown that the second blocks $\omega \bar{\mathbf{L}}_\tau$ and $\omega \bar{\mathbf{J}}_\tau$ of matrices $\omega \hat{\mathbf{L}}_s$ and $\omega \hat{\mathbf{J}}_s$ and the second blocks $\omega \bar{\mathbf{T}}_s$, $\omega \bar{\mathbf{V}}_s$ and $\omega \bar{\mathbf{K}}_\tau$ of vectors $\omega \hat{\mathbf{I}}_s$, $\omega \hat{\mathbf{V}}_s$ and $\omega \hat{\mathbf{K}}_\tau$ are complex conjugate terms which are not essential to describe the dynamics of the system. From these considerations it follows that a complex and reduced model of the multi-phase PMSM expressed in a new frame $\bar{\Sigma}_\omega$ can be obtained using a state space pseudo-transformation ${}^t\mathbf{I}_s = \Re({}^t\bar{\mathbf{T}}_{\omega N} \omega \bar{\mathbf{I}}_s)$ based on the following complex rectangular matrix ${}^t\bar{\mathbf{T}}_{\omega N} \in \mathbb{C}^{m_s \times \frac{m_s+1}{2}}$:

$${}^t\bar{\mathbf{T}}_{\omega N} = {}^t\bar{\mathbf{T}}_\omega \mathbf{N} = [{}^t\bar{\mathbf{T}}_\omega \mathbf{z}_{m_s}] \mathbf{N} \quad (22)$$

where ${}^t\bar{\mathbf{T}}_\omega$ is the matrix defined in (16) and \mathbf{z}_{m_s} is the vector defined in (6). When the stator phases are star-connected, the last column of matrices ${}^t\bar{\mathbf{T}}_\omega$ and \mathbf{N} can be eliminated and matrix ${}^t\bar{\mathbf{T}}_{\omega N}$ reduces to the rectangular matrix $\sqrt{2}{}^t\bar{\mathbf{T}}_\omega$. For a five-phase motor the matrices ${}^t\bar{\mathbf{T}}_\omega$ and \mathbf{N} have the following form:

$${}^t\bar{\mathbf{T}}_\omega = \frac{1}{\sqrt{5}} \begin{bmatrix} e^{j\theta} & e^{j3\theta} & 1 \\ e^{j(\theta-\gamma_s)} & e^{j3(\theta-\gamma_s)} & 1 \\ e^{j(\theta-2\gamma_s)} & e^{j3(\theta-2\gamma_s)} & 1 \\ e^{j(\theta-3\gamma_s)} & e^{j3(\theta-3\gamma_s)} & 1 \\ e^{j(\theta-4\gamma_s)} & e^{j3(\theta-4\gamma_s)} & 1 \end{bmatrix}, \quad \mathbf{N} = \begin{bmatrix} \sqrt{2} & 0 & 0 \\ 0 & \sqrt{2} & 0 \\ 0 & 0 & 1 \end{bmatrix}.$$

Applying the pseudo-transformation ${}^t\mathbf{I}_s = \Re({}^t\bar{\mathbf{T}}_{\omega N} \omega \bar{\mathbf{I}}_s)$ to system (3), one obtains the following transformed system $\bar{\mathcal{S}}_\omega$ expressed in the complex and reduced rotating frame $\bar{\Sigma}_\omega$:

$$\begin{bmatrix} \omega \bar{\mathbf{L}}_s & \mathbf{0} \\ \mathbf{0} & J_m \end{bmatrix} \begin{bmatrix} \omega \dot{\bar{\mathbf{I}}}_s \\ \dot{\omega}_m \end{bmatrix} = - \begin{bmatrix} \omega \bar{\mathbf{R}}_s + \omega \bar{\mathbf{L}}_s \omega \bar{\mathbf{J}}_s & \omega \bar{\mathbf{K}}_{\tau N} \\ -\omega \bar{\mathbf{K}}_{\tau N}^* & b_m \end{bmatrix} \begin{bmatrix} \omega \bar{\mathbf{I}}_s \\ \omega_m \end{bmatrix} + \begin{bmatrix} \omega \bar{\mathbf{V}}_s \\ -\tau_e \end{bmatrix} \quad (23)$$

m_s	Dynamic model
3	$\begin{bmatrix} L_{s1} & 0 \\ 0 & J_m \end{bmatrix} \begin{bmatrix} \omega \dot{\mathbf{I}}_{s1} \\ \dot{\omega}_m \end{bmatrix} = - \begin{bmatrix} R_s + jp\omega_m L_{s1} & jp\varphi_c \sqrt{\frac{3}{2}} a_1 \\ -jp\varphi_c \sqrt{\frac{3}{2}} a_1 & b_m \end{bmatrix} \begin{bmatrix} \omega \mathbf{I}_{s1} \\ \omega_m \end{bmatrix} + \begin{bmatrix} \omega \mathbf{V}_{s1} \\ -\tau_e \end{bmatrix}$
5	$\begin{bmatrix} L_{s1} & 0 & 0 \\ 0 & L_{s3} & 0 \\ 0 & 0 & J_m \end{bmatrix} \begin{bmatrix} \omega \dot{\mathbf{I}}_{s1} \\ \omega \dot{\mathbf{I}}_{s3} \\ \dot{\omega}_m \end{bmatrix} = - \begin{bmatrix} R_s + jp\omega_m L_{s1} & 0 & jp\varphi_c \sqrt{\frac{5}{2}} a_1 \\ 0 & R_s + j3p\omega_m L_{s3} & jp\varphi_c \sqrt{\frac{5}{2}} 3a_3 \\ -jp\varphi_c \sqrt{\frac{5}{2}} a_1 & -jp\varphi_c \sqrt{\frac{5}{2}} 3a_3 & b_m \end{bmatrix} \begin{bmatrix} \omega \mathbf{I}_{s1} \\ \omega \mathbf{I}_{s3} \\ \omega_m \end{bmatrix} + \begin{bmatrix} \omega \mathbf{V}_{s1} \\ \omega \mathbf{V}_{s3} \\ -\tau_e \end{bmatrix}$

Figure 9 Dynamic models of a star-connected multi-phase PMSM in the reduced complex rotating frame $\bar{\Sigma}_\omega$ for $m_s = 3$ and $m_s = 5$.

where vectors $\omega \mathbf{I}_s$, $\omega \mathbf{V}_s$ and $\omega \mathbf{K}_{\tau N}$ are obtained using matrix ${}^t \mathbf{T}_{\omega N}$:

$$\omega \mathbf{I}_s = {}^t \mathbf{T}_{\omega N}^* {}^t \mathbf{I}_s = \begin{bmatrix} \omega \mathbf{I}_s \\ \omega_{I_{sm_s}} \end{bmatrix}, \omega \mathbf{V}_s = {}^t \mathbf{T}_{\omega N}^* {}^t \mathbf{V}_s = \begin{bmatrix} \omega \mathbf{V}_s \\ \omega_{V_{sm_s}} \end{bmatrix}, \omega \mathbf{K}_{\tau N} = {}^t \mathbf{T}_{\omega N}^* {}^t \mathbf{K}_\tau = \begin{bmatrix} \omega \mathbf{K}_\tau \\ \omega_{K_{\tau m_s}} \end{bmatrix}$$

and matrices $\omega \mathbf{L}_s$, $\omega \mathbf{J}_s$ and $\omega \mathbf{R}_s$ are obtained using matrix ${}^t \mathbf{T}_\omega$:

$$\omega \mathbf{L}_s = {}^t \mathbf{T}_\omega^* {}^t \mathbf{L}_s {}^t \mathbf{T}_\omega = \begin{bmatrix} \omega \mathbf{L}_s & \mathbf{0} \\ \mathbf{0} & L_{s0} \end{bmatrix}, \omega \mathbf{J}_s = {}^t \mathbf{T}_\omega^* {}^t \dot{\mathbf{T}}_\omega = \begin{bmatrix} \omega \mathbf{J}_s & \mathbf{0} \\ \mathbf{0} & 0 \end{bmatrix}, \omega \mathbf{R}_s = {}^t \mathbf{T}_\omega^* {}^t \mathbf{R}_s {}^t \mathbf{T}_\omega = R_s \mathbf{I}_{\frac{m_s+1}{2}}$$

Note that these square matrices have dimension $(m_s+1)/2$, while the square matrices $\omega \hat{\mathbf{L}}_s$ and $\omega \hat{\mathbf{J}}_s$ in (18) and vectors $\omega \hat{\mathbf{I}}_s$ and $\omega \hat{\mathbf{V}}_s$ in (19) have dimension m_s . As a matter of fact, using the pseudo-transformation ${}^t \mathbf{I}_s = \Re \mathfrak{e} ({}^t \mathbf{T}_{\omega N} \omega \mathbf{I}_s)$ the original m_s -dimension model in the fixed frame Σ_t is transformed and reduced to a $(m_s-1)/2$ -dimension complex model in the transformed reduced rotating frame $\bar{\Sigma}_\omega$. When the rotor flux function $\bar{\phi}(\theta)$ has the structure defined in (12) the torque vector $\omega \mathbf{K}_{\tau N}$ has a complex and constant form:

$$\omega \mathbf{K}_{\tau N}(\theta) = \omega \mathbf{K}_{\tau N} = jp\varphi_c \sqrt{\frac{m_s}{2}} \begin{bmatrix} k \\ \ll ka_k \gg \\ 1:2:m_s-2 \\ 0 \end{bmatrix}.$$

The POG scheme corresponding to the dynamic system $\bar{\mathcal{S}}_\omega$ given in (23) is shown in Fig. 8. The *connection blocks* between the power sections ①-① and ②-③ take into account the function $\Re \mathfrak{e}(\cdot)$ which is present in relation (21). The mechanical part of the scheme is unchanged, while the internal variables of the electrical part (between power sections ① and ③) are complex vectors of reduced dimension. The dynamic models of a star-connected multi-phase PMSM in the reduced complex rotating frame $\bar{\Sigma}_\omega$ for $m_s = 3$ and $m_s = 5$ are shown in Fig. 9.

Remark: it can be easily shown that system (23) can also be obtained from system

(7) using the bijective correspondences between two-dimensional vectors, complex numbers and two-dimensional matrices:

$$\begin{bmatrix} \alpha \\ \beta \end{bmatrix} \leftrightarrow \alpha + j\beta \leftrightarrow \begin{bmatrix} \alpha & -\beta \\ \beta & \alpha \end{bmatrix}. \quad (24)$$

The transformation ${}^t\bar{\mathbf{T}}_\omega$ is similar to the matrix proposed in the *Space Vector approach*, see Grandi et al. (2006) and Casadei et al. (2008), which is based on the following transformation matrix:

$${}^t\mathbf{S}_\omega^* = \frac{2}{m_s} \begin{bmatrix} & & h \\ & \begin{bmatrix} 1 & 1 \end{bmatrix} & \\ & & 1:m_s \\ k & \begin{bmatrix} e^{j(h-1)k\gamma_s} & \dots & e^{jh\gamma_s} \end{bmatrix} & h \\ 1:2:m_s-1 & & 1:m_s \end{bmatrix} = \frac{2}{5} \begin{bmatrix} 1 & 1 & 1 & 1 & 1 \\ 1 & e^{j\gamma_s} & e^{j2\gamma_s} & e^{j3\gamma_s} & e^{j4\gamma_s} \\ 1 & e^{j3\gamma_s} & e^{j6\gamma_s} & e^{j9\gamma_s} & e^{j12\gamma_s} \end{bmatrix} \frac{1}{m_s}.$$

System \bar{S}_ω is described by complex variables and is obtained using the rectangular pseudo-transformation matrix ${}^t\bar{\mathbf{T}}_{\omega N}$. For this reason the dimension of the transformed vectors is reduced and system \bar{S}_ω has a very compact form. The *direct* and *quadrature* variables are still available. The characteristic polynomial $p(s)$ of the linearized system \bar{S}_ω has complex coefficients. The eigenvalues of system \bar{S}_ω coincide with the complex roots of the characteristic polynomial $p(s)$ and their complex conjugate values. The pseudo-transformation matrix ${}^t\bar{\mathbf{T}}_{\omega N}$ is *power-invariant*. Indeed it can be easily proved that the instantaneous power $p(t) = {}^t\mathbf{V}_s^T {}^t\mathbf{I}_s$ in section ① in Fig. 8 is equal to the real part of the complex instantaneous power $s(t) = \omega \bar{\mathbf{V}}_s^* \bar{\mathbf{I}}_s$ in section ①:

$$\begin{aligned} p(t) &= {}^t\mathbf{V}_s^T {}^t\mathbf{I}_s = {}^t\mathbf{V}_s^T \Re({}^t\bar{\mathbf{T}}_{\omega N} {}^t\bar{\mathbf{T}}_{\omega N}^* {}^t\mathbf{I}_s) \\ &= \Re({}^t\mathbf{V}_s^T {}^t\bar{\mathbf{T}}_{\omega N} {}^t\bar{\mathbf{T}}_{\omega N}^* {}^t\mathbf{I}_s) = \Re(\omega \bar{\mathbf{V}}_s^* \bar{\mathbf{I}}_s) = \Re(s(t)). \end{aligned}$$

The Space Vector approach is *not power-invariant*, indeed the instantaneous power $p(t) = {}^t\mathbf{V}_s^T {}^t\mathbf{I}_s$ is not equal (but proportional) to the real part of the complex power $s(t) = {}^S\mathbf{V}_s^* {}^S\mathbf{I}_s$:

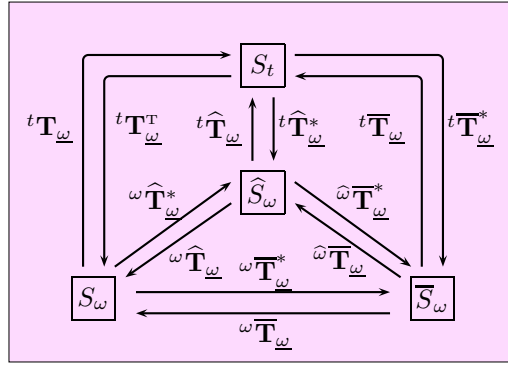
$$p(t) = m_s \Re(s(t)) = m_s \Re({}^S\mathbf{V}_s^* {}^S\mathbf{I}_s).$$

4.4 Comparison among the proposed transformations

The three state space transformations presented in the previous sections have been applied to system S_t obtaining three different dynamic systems S_ω , \hat{S}_ω and \bar{S}_ω which are equivalent from a mathematical point of view. The main features of the proposed transformations are summarized in Table 2. It is possible to pass from one dynamic model to the others using the transformation matrices shown in Fig. 10. The three transformation matrices ${}^\omega\hat{\mathbf{T}}_\omega$, ${}^\omega\bar{\mathbf{T}}_\omega$ and ${}^\omega\mathbf{T}_\omega$ which link together the dynamic systems S_ω , \hat{S}_ω and \bar{S}_ω are related to matrices ${}^t\mathbf{T}_\omega$, ${}^t\hat{\mathbf{T}}_\omega$ and ${}^t\bar{\mathbf{T}}_\omega$ as follows:

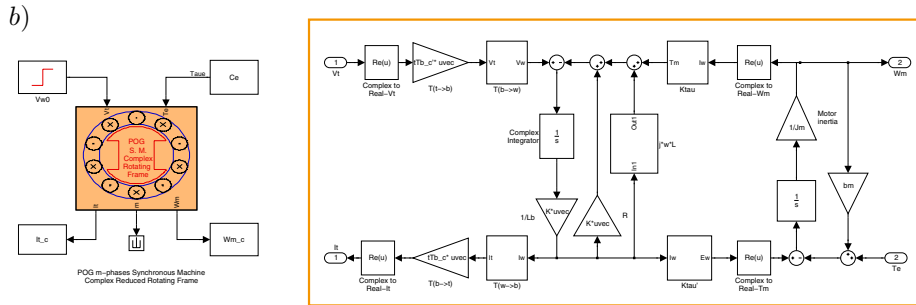
$${}^\omega\hat{\mathbf{T}}_\omega = {}^t\mathbf{T}_\omega^T {}^t\hat{\mathbf{T}}_\omega, \quad {}^\omega\bar{\mathbf{T}}_\omega = {}^t\hat{\mathbf{T}}_\omega^* {}^t\bar{\mathbf{T}}_\omega, \quad {}^\omega\mathbf{T}_\omega = {}^t\mathbf{T}_\omega^T {}^t\mathbf{T}_\omega$$

System		S_t	S_ω	\hat{S}_ω	\bar{S}_ω
Transformations		none	${}^t\mathbf{T}_\omega$	${}^t\hat{\mathbf{T}}_\omega$	${}^t\bar{\mathbf{T}}_\omega$
Power invariant		/	Yes	Yes	Yes
Variables	type	real time variant	real constant	complex constant	complex constant
	dimension	m_s	m_s	m_s	$\frac{m_s+1}{2}$
Fictitious machines		/	$\frac{m_s-1}{2}$	$\frac{m_s-1}{2}$	$\frac{m_s-1}{2}$

Table 2 Main features of the proposed transformations.**Figure 10** Transformation matrices relating the systems S_t , S_ω , \hat{S}_ω and \bar{S}_ω .

5 Simulation

All the POG models of a multi-phase PMSM shown from Fig. 3 to Fig. 8 and the model with Park transformation of Fig. 6 have been implemented in Simulink. The Simulink scheme reported in Fig. 11 is the implementation of the POG model shown in Fig. 8. It has a vectorial structure that do not need to consider the fictitious machines. The Simulink scheme of the electric motor is shown in Fig. 11.a: the masked block contains the Simulink scheme of Fig. 11.b. Thanks to the graphical interface, the user can modify the number of phases and other parameters of the

**Figure 11** Simulink schemes: a) Simulink scheme of the controlled electric motor, b) Simulink scheme of a multi-phase electrical motor in the frame Σ_ω .

model without changing the structure of the model.

The simulation results shown in this section have been obtained considering a five-phase star connected motor with the parameters given in Shan et al. (2006). The electrical and mechanical parameters are: $m_s=5$, $p=8$, $R_s=0.11\ \Omega$, $L_s=2.1\ \text{mH}$, $M_{s0}=0.7\ \text{mH}$, $\varphi_r=0.0025\ \text{Wb}$, $J_m=1.6\ \text{kg m}^2$, $b_m=2.06\ \text{Nm s/rad}$, $a_1=0.71$, $a_3=0.04$ and the external torque $\tau_e=0\ \text{Nm}$. Three different models are compared:

- 1) POG model in the rotating frame Σ_ω ,
- 2) Park model,
- 3) POG model in the reduced complex rotating frame $\bar{\Sigma}_\omega$.

The aim of the paper is to propose new dynamic models for the multi-phase PMSM, so no advanced controls are investigated and the systems are fed with the following step input in order to see the open-loop step response of the motors:

- 1) ${}^t\mathbf{V}_{sd} = {}^t\mathbf{T}_\omega {}^\omega\mathbf{V}_{sd} = {}^t\bar{\mathbf{T}}_\omega \left(({}^\omega\mathbf{R}_s + {}^\omega\mathbf{J}_s {}^\omega\mathbf{L}_s) {}^\omega\mathbf{I}_d + {}^\omega\mathbf{K}_\tau \omega_{md} \right)$
- 2) ${}^t\mathbf{V}_{sd} = {}^t\mathbf{P}_\omega {}^P\mathbf{V}_{sd} = \sqrt{\frac{m_s}{2}} {}^t\mathbf{T}_\omega \left(({}^\omega\mathbf{R}_s + {}^\omega\mathbf{J}_s {}^\omega\mathbf{L}_s) {}^P\mathbf{I}_d + \sqrt{\frac{2}{m_s}} {}^\omega\mathbf{K}_\tau \omega_{md} \right)$
- 3) ${}^t\mathbf{V}_{sd} = \Re\left({}^t\bar{\mathbf{T}}_{\omega N} {}^\omega\bar{\mathbf{V}}_{sd}\right) = \Re\left({}^t\bar{\mathbf{T}}_{\omega N} \left[({}^\omega\bar{\mathbf{R}}_s + {}^\omega\bar{\mathbf{J}}_s {}^\omega\bar{\mathbf{L}}_s) {}^\omega\bar{\mathbf{I}}_d + {}^\omega\bar{\mathbf{K}}_\tau \omega_{md} \right] \right)$

These equations are obtained using the POG schemes in Fig. 4, Fig. 5 and Fig. 8 starting from the three desired current vectors ${}^\omega\bar{\mathbf{I}}_d$, ${}^P\mathbf{I}_d$, ${}^\omega\bar{\mathbf{I}}_d$ and the desired motor velocity ω_{md} . The desired current vectors, according to Shan et al. (2006), are:

- 1) ${}^\omega\mathbf{I}_d = [0\ 23.72\ 0\ 5.93]^\top [A]$
- 2) ${}^P\mathbf{I}_d = \sqrt{\frac{2}{5}} {}^\omega\mathbf{I}_d = [0\ 15\ 0\ 3.75]^\top [A]$
- 3) ${}^\omega\bar{\mathbf{I}}_d = j[23.72\ 5.93]^\top [A]$.

The time behaviors of the motor velocity ω_m and motor torque τ_m are shown in Fig. 12. The motors accelerate from 0 to the desired velocity $\omega_d = 21.55\ [\text{rad/s}]$ and in steady-state condition the PMSM generates the desired torque $\tau_m = \tau_d = 44.4\ \text{Nm}$. The overshoot in the torque response disappears when a closed-loop control is used instead of the open-loop control. In Fig. 13 one can see the first phase current I_{s1} in the steady state condition with its spectrum. It is clear that also the 3-rd harmonic is injected. The order of the error between the three simulation results is 10^{-14} . Using (24) it is possible to rewrite the real vector $[{}^P I_{dk}\ {}^P I_{qk}]$ as a complex vector ${}^P\bar{\mathbf{I}}_{sk} = {}^P I_{dk} + j {}^P I_{qk}$. The current vectors ${}^P\bar{\mathbf{I}}_{sk}$ and ${}^\omega\bar{\mathbf{I}}_{sk}$ in the two-dimensional subspaces $\bar{\Sigma}_{\omega k}$ are shown in Fig. 14 on a complex plane. During the transient the vectors ${}^P\bar{\mathbf{I}}_{s1}$ and ${}^\omega\bar{\mathbf{I}}_{s1}$ in the complex subspaces $\bar{\Sigma}_{\omega 1}$ and the vectors ${}^P\bar{\mathbf{I}}_{s3}$ and ${}^\omega\bar{\mathbf{I}}_{s3}$ in the complex subspaces $\bar{\Sigma}_{\omega 3}$ describe a trajectory due to the step-response, so both the direct and quadrature components are different from zero. In steady-state condition the direct components are equal to zero, so the complex vectors ${}^P\bar{\mathbf{I}}_{s1}$ and ${}^\omega\bar{\mathbf{I}}_{s1}$ are on the imaginary axis. Note that, according to (15), it holds that ${}^P\bar{\mathbf{I}}_{sk} = \sqrt{\frac{2}{5}} {}^\omega\bar{\mathbf{I}}_{sk}$.

In Shan et al. (2006) the harmonics amplitude are not tied to the harmonic spectrum of the rotor flux (the amplitude of the 3-rd harmonic is 25% of the fundamental one, see Fig. 13). Consequently the previous desired current vectors do not minimize the dissipating power.

Since the motor torque τ_m is obtained as the scalar product between the transformed torque and current vectors $\tau_m = {}^\omega\bar{\mathbf{K}}_\tau {}^\omega\bar{\mathbf{I}}_s$, then the desired current

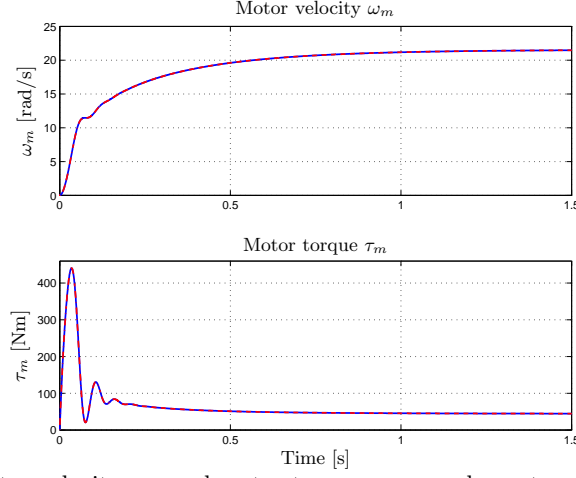


Figure 12 Motor velocity ω_m and motor torque τ_m open-loop step response.

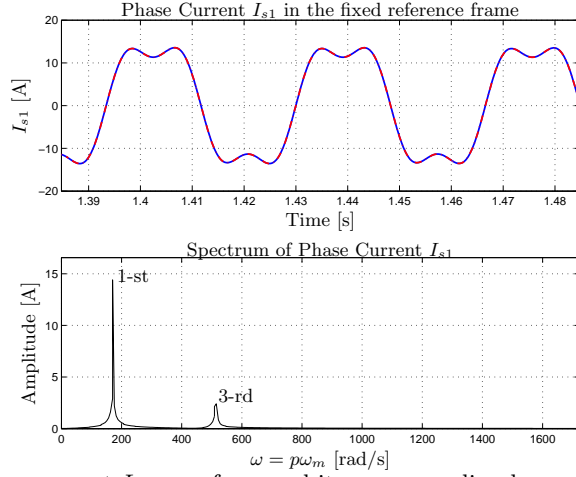


Figure 13 Phase current I_{s1} waveform and its corresponding harmonic spectrum in steady-state condition.

vector ${}^\omega \bar{\mathbf{I}}_d$ which provides the desired torque τ_d minimizing the power dissipation is the vector with the minimum modulus parallel to the transformed torque vector. Using this vectorial notation it is evident that the optimal current vector that provides the desired torque τ_d minimizing the dissipation is:

$${}^\omega \bar{\mathbf{I}}_{do} = \frac{{}^\omega \bar{\mathbf{K}}_\tau}{|{}^\omega \bar{\mathbf{K}}_\tau|^2} \tau_d = \left\| \left[j \tilde{K}_k \right]_{1:2:m_s-2}^k \right\| \tau_d, \quad \tilde{K}_k = \frac{K_{qk}}{|{}^\omega \bar{\mathbf{K}}_\tau|^2} = \frac{ka_k}{p\varphi_c \sqrt{\frac{m_s}{2}} \sum_{k=1:2}^{m_s-2} (ka_k)^2}$$

where the distribution coefficients \tilde{K}_k relate the harmonics amplitude of the injected harmonics with the harmonic spectrum of the rotor flux.

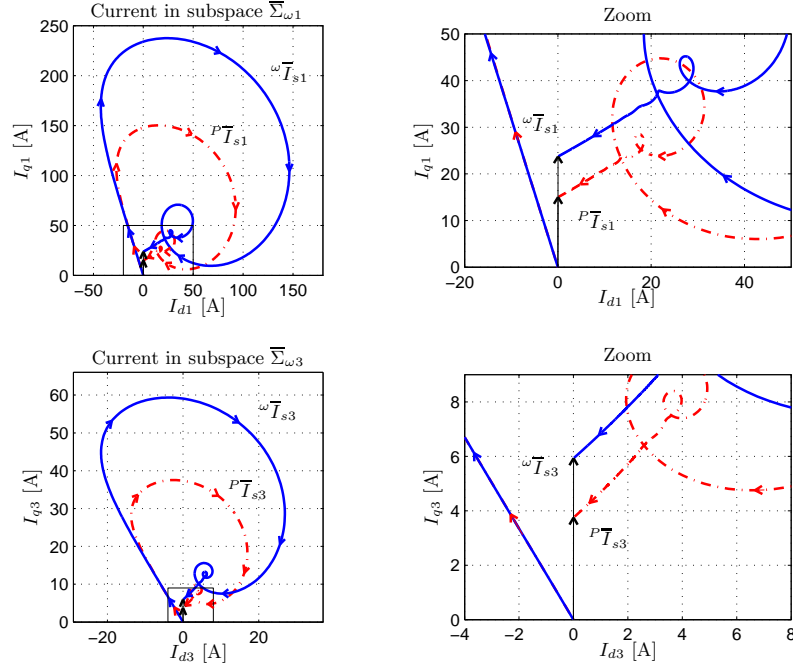


Figure 14 Current vectors $P \bar{T}_{sk}$ (red dashed) and $\omega \bar{T}_{sk}$ (blue solid) in the two-dimensional subspaces Σ_{ω_k} .

In our case the optimal current vector is $\omega \mathbf{I}_{do} = [0 \ 24.03 \ 0 \ 4.06]^T$ [A]. The comparison between the first phase current I_{s1} in the steady state condition obtained using the vectors $\omega \bar{\mathbf{I}}_d$ (red dashed) and the vectors $I_{so1} \ \omega \bar{\mathbf{I}}_{do}$ (blue solid) are shown in Fig. 15.

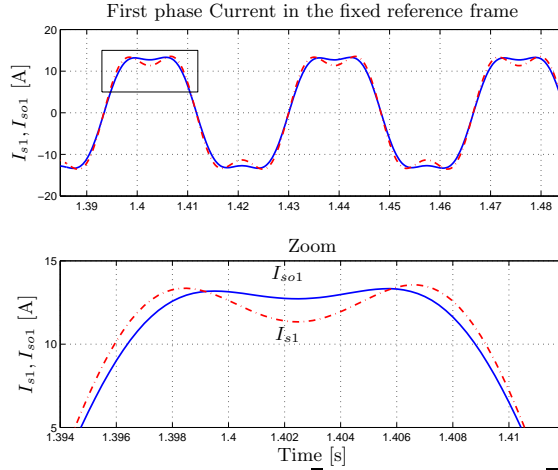


Figure 15 First phase current for vectors $\omega \bar{\mathbf{I}}_d$ (red dashed) and $\omega \bar{\mathbf{I}}_{do}$ (blue solid) in the fixed reference frame Σ_t .

6 Conclusion

In this paper the modeling of multi-phase PMSM with an odd number of star-connected phases has been investigated. The dynamic model of the motor has been proposed as general as possible and for an arbitrary shape of rotor flux. Three different state space transformations, one real and two complex, have been proposed. Each transformation has been analyzed in detail and compared with the classical transformations known in the literature. The proposed transformations have some advantages with respect to those used in the literature: they are *power-invariant* and they use a very compact vectorial notation. In particular the transformation ${}^t\overline{\mathbf{T}}_{\omega N}$, which allows to express the dynamics of the system with respect to a complex and reduced rotating frame $\overline{\Sigma}_{\omega}$, seems to be the best one because it provides a complex dynamic model with a reduced dimension of the state space vectors: only $(m_s+1)/2$ complex variable are used. The reported simulation results show the effectiveness of the proposed dynamic models.

The exploitations of the POG schemes with vectorial notation has the important advantage that they can be directly implemented in Simulink, they are a complete and exact dynamical description of the considered system and there is no need to consider separate fictitious machines. The model is the same whatever the number of phases is and there is no need to rebuild the model when m_s changes. Using this model some advanced control can be developed taking advantage from the compact vectorial notation. Moreover the proposed model can be extended also in the case of open-phase fault condition thus being very useful for testing in simulation some new fault-tolerant control strategies.

References

- White D.C. and Woodson H. H. , “ Electromechanical Energy Conversion”, *New York: Wiley*, 1959.
- Levi E. , “Multiphase Electric Machines for Variable-Speed Applications” *IEEE Transactions on Industrial Electronics*, vol.55, no.5, pp.1893-1909, May 2008.
- Parsa L., “On advantages of multi-phase machines” *31st Annual Conference of IEEE Industrial Electronics Society*, IECON 2005.
- Parsa L. and Toliyat H.A. , “Five-Phase Permanent-Magnet Motor Drives”, *IEEE Transactions on Industry Applications* , 2005, Vol. 41, No. 1, pp. 30-37.
- Kestelyn X., Semail E., Hautier JP. , “Vectorial Multi-machine Modeling for a Five-Phase Machine”, in Proc. Int. Conf. Electrical Machines (ICEM), Bruges, Belgium, 2002, CD-ROM, Paper 394.
- Semail E. , Kestelyn X. , Bouscayrol A., “Right Harmonic Spectrum for the Back-Electromotive Force of a n -phase Synchronous Motor”, *39th Annual Meeting of Industry Applications Conference*, IAS 2004, ISBN: 0-7803-8486-5.
- Paap G.C. , “Symmetrical Components in the Time Domain and Their Application to Power Network Calculations”, *IEEE Transactions on Power Systems* , Volume 15, Issue 2, pp.522-528, 2000.
- Toliyat H.A. , Rahimian M.M. , Lipo T.A. , “dq Modeling of Five Phase Synchronous Reluctance Machines Including Third Harmonic of Air-Gap MMF”, *Industry Applications Society Annual Meeting* , 1991., Conference Record of the 1991 IEEE pp. 231-237 vol.1.

- Figuerola J. , Cros J. and Viarouge P. , “Generalized Transformations for Polyphase Phase-Modulation Motors”, *IEEE Transactions on Energy Conversion* , 2006, Vol. 21, No. 2, pp. 332-341.
- Kang M. , Huang J. , Yang J. , Liu D. , H. Jiang, “Strategies for the fault-tolerant current control of a multiphase machine under open phase conditions”, *International Conference on Electrical Machines and Systems*, ICEMS 2009.
- Fortescue C.L. , “Method of Symmetrical Coordinates Applied to the Solution of Polyphase Networks.” *Trans. AIEE* , pt. II, vol. 37, pp.1027-1140, 1918.
- Grandi G. , Serra G. , Tani A. , “General Analysis of Multi-Phase Systems Based on Space Vector Approach”, *Power Electronics and Motion Control Conference* , EPE-PEMC 2006, pp.834-840, 2006.
- Clarke E. (1950) *Circuit Analysis of AC Power System*, New York: Wiley, 1950, vol.I.
- Park R. H. (1929) *Two-reaction theory of synchronous machines*, *Trans. AIEE* , vol. 48, pp. 716, 1929.
- Vas P. (1990) *Vector Control of AC Machines*, Oxford University Press, 1990.
- Leonhard W., *Control of Electrical Drives*, 3rd Edition 2001, Springer-Verlag Berlin Heidelberg NewYork, ISBN 3-540-41820-2.
- Zanasi R., Grossi F., “Multi-phase Synchronous Motors: POG Modeling and Optimal Shaping of the Rotor Flux”, *Proceedings of ELECTRIMACS 2008*, Québec, Canada, June 2008.
- Zanasi R., Grossi F., “Optimal Rotor Flux Shape for Multi-phase Permanent Magnet Synchronous Motors”, *Proceedings of International Power Electronics and Motion Control Conference*, September 1-3 2008, Poznan, Poland.
- Zanasi R., “Power Oriented Modelling of Dynamical System for Simulation”, *Proceedings of IMACS Symp. on Modelling and Control of Technological System*, Lille, France, May 1991.
- Zanasi R., “The Power-Oriented Graphs Technique: system modeling and basic properties”, *Proceedings of Vehicular Power and Propulsion Conference*, Lille, France, Sept 2010.
- Shan X., Xuhui W., Zhao F., “Multiphase Permanent Magnet Motor Drive System Based on A Novel Multiphase SVPWM”, *Proceedings of CES/IEEE 5th International Power Electronics and Motion Control Conference IPEMC*, 2006, vol.1, pp.1-5.
- Aller J.M., Bueno A., Paga T., “Power System Analysis Using Space-Vector Transformation”, *IEEE Transactions on Power Systems*, Vol. 17, No. 4, pp. 957-965, 2002.
- Casadei D., Dujic D., Levi E., Serra G., Tani A., Zarri L., “General Modulation Strategy for Seven-Phase Inverters With Independent Control of Multiple Voltage Space Vectors”, *IEEE Transactions on Industrial Electronics*, vol.55, no.2, pp.1921 - 1932, 2008.